

Mitigating Write Disturbance Errors of Phase-Change Memory as In-Module Approach

Hyokeun Lee*, Seungyong Lee*, Byeongki Song*, Moonsoo Kim*, Seokbo Shim‡, Hyun Kim†, Hyuk-Jae Lee*

*Seoul National University, Seoul, {hklee, sylee, kimms213, bksong, hyuk_jae_lee}@capp.snu.ac.kr

†Seoul National University of Science and Technology, Seoul, hyunkim@seoultech.ac.kr

‡SK Hynix, Icheon, seokbo.shim@sk.com

Abstract—With the growing demand for technology scaling and storage capacity in server systems to support high-performance computing, phase-change memory (PCM) has garnered attention as the next-generation non-volatile memory to satisfy these requirements. However, write disturbance error (WDE) appears as a serious reliability problem preventing PCM from general commercialization. WDE occurs on the neighboring cells of a written cell due to heat dissipation. Previous studies for the prevention of WDEs are based on the write cache or verify-and-correction while they often suffer from significant area overhead and performance degradation, making it unsuitable for high-performance computing. Therefore, an on-demand correction is required to minimize the performance overhead. In this paper, an in-module disturbance barrier (IMDB) mitigating WDEs is proposed. IMDB includes two sets of SRAMs into two levels and evicts entries with a policy that leverages the characteristics of WDE. In this work, the comparator dedicated to the replacement policy requires significant hardware resources and latency. Thus, an approximate comparator is designed to reduce the area and latency considerably. Furthermore, the exploration of architecture parameters is conducted to obtain cost-effective design. The proposed work significantly reduces WDEs without a noticeable speed degradation and additional energy consumption compared to previous methods.

I. INTRODUCTION

Phase-change memory (PCM) gains attention as the next-generation non-volatile memory (NVM) device to replace the existing DRAM-based main memory system or to introduce a new storage-class memory layer between DRAM and storage, owing to its non-volatility, latency, and scalability [30], [32]. In recent years, software-defined memory has been proposed to utilize the NVM as a high-speed storage or expanded main memory interchangeably on user-level applications [11], [12], [18], [57]. On the other hand, applications of in-memory database require data to be persisted with lower latency in persistent memories; hence, PCM is an adequate candidate for this purpose [6], [8], [15], [22], [24], [31], [56], [76]. Moreover, products based on PCM have been tested on various environments for performance evaluation and exploration of their suitable applications [26], [37], [40], [41], [65], [66], [69]. Therefore, leveraging and enhancing the PCM-related technology is crucial to attaining a low-latency and large-scale memory system in the future.

Even though PCM has attractive characteristics, it is not ready for steady commercialization due to lower cell reliability than DRAM [58]. There are several kinds of reliability issues in PCM, such as cell endurance [5], [9], [10], [14], [19],

[43], [46], [52], [53], [54], [60], [61], [62], [68], [71], [72], [73], [74], resistance drift [1], [16], [29], [55], [67], [70], [75], and read/write disturbance [3], [17], [21], [23], [35], [39], [48], [50], [51], [59], [63], [64]. Write disturbance error (WDE) is one of the major problems, which delays its massive commercialization [17], [21], [23], [59], [64]. WDE is an interference problem on adjacent cells similar to row-hammer in DRAM devices [27], [28], [33], [38], [47], [49]. However, unlike DRAM row-hammer, it especially occurs on an idle cell near to a cell under reset, thus changes the state of an idle cell and reading an incorrect value. This problem must be addressed as the highest priority because it would be exacerbated as the technology scales down [59]. Additionally, a widely-used application such as in-memory database directly stores data in an NVM, which heavily utilizes cache-line flush instructions [22], [24], [31], [56], [76]. This kind of application would incur frequent write operations on PCM and thereby making cells be vulnerable to WDEs.

Previously, existing techniques for mitigating WDEs, such as *DIN*, *Lazy correction*, and *ADAM*, are built on top of verify-and-correction (VnC), which significantly degrades performance and consequently hinders the implementation of high-performance computing platforms [23], [59], [64]. Meanwhile, a solution for WDEs, the write cache-based method [21], rarely considers the size limit of a supercapacitor, which is required for data flush on a system crash or failure (up to 100us hold-up time for commercial devices) [20].

To avoid these disadvantages (i.e., performance degradation and additional hardware resource), this paper proposes a low-cost in-module write disturbance barrier (IMDB). Previous solutions are built upon the probability-based WDE trigger model, which incur WDEs for specific probabilities as in [23], [59], [64]; however, it is recently reported that the WDE occurs when the cells are exposed to RESET operation for specific times [21]. Therefore, the proposed method records the number of 1-to-0 bit flips (i.e., the number of RESET), by which most of the WDE-vulnerable data can be rewritten right before 1-to-0 bit flips reach the disturbance limitation. Most of the data are not recorded not only for managing more write addresses in the SRAM-based table but also for a smaller supercapacitor area required for system failure, except for a higher-tier second table, named *barrier buffer*, to minimize the additional hardware resource. Meanwhile, if the replacement policy merely regards the entry holding a smaller number of

1-to-0 flips as an eviction candidate, it would overlook the temporal locality; hence, it would easily evict the insufficiently baked addresses that may incur WDEs to other cells in the near-future. Thus, a simple prior knowledge is provided to overcome such a challenging point. Furthermore, the policy may require to read multiple counting information on the table at once and compares the numbers. It expands the number of read ports on SRAM and thereby incurs a significant amount of energy, latency, and area. Therefore, an approximate lowest number estimator (*AppLE*), which probabilistically compares numbers based on the sampling method, is proposed to reduce additional latency and area.

The experimental results indicate that the proposed method reduces WDEs by $1218\times$, $439\times$, $202\times$ in comparison with *ADAM*, *lazy correction*, *SIWC-entry*, respectively, with negligible speed degradation. In particular, the following challenging issues are resolved in this study:

- A low-cost on-demand rewrite method assisted by a two-tier SRAM is proposed to mitigate WDE. This is the first attempt of on-demand approach based on more practical WDE trigger model to reduce WDEs.
- The replacement policy regards the number of 1-to-0 flips as an eviction criterion, which may frequently evict the newly inserted entry once the table is full. This paper introduces a novel prior knowledge offering method to tackle this problem.
- The replacement policy requires multiple read ports on SRAM that incurs considerable overhead. This paper designs a probabilistic comparator hardware to highly reduce the number of read ports on SRAM and enhance the feasibility of the proposed method.
- Several design parameters are required in the proposed method; hence, sensitivity analyses are conducted to acquire cost-effective design in the evaluation section.

II. BACKGROUND

A. Introduction to Phase-Change Memory

PCM is a resistive memory device composed of GST materials that exploit two material states, namely *amorphous* and *crystalline*, to program cells with heat. The amorphous state is achieved by heating the bottom electrode of the device to 600 degree Celsius for a short time, by which the cell resistance is increased (i.e., RESET). On the other hand, the crystalline state is achieved by supplying 300 degrees Celsius for a longer time compared with the amorphous state [4], [34], [77]. The data stored in a PCM can be simultaneously sensed by supplying a sensing voltage to the cells; hence, the read latency is much shorter than the write latency [45].

A detailed overview of the PCM device in an 8GB module is illustrated in Figure 2(a). The device consists of eight subarrays, and each subarray is composed of eight MATs (8K wordlines and 4K bitlines for each MAT). First of all, main wordline drivers activate a subarray in each bank, and the row address is commonly fed into sub-wordline drivers (SWD) in the activated subarray for selecting a row that carries 4Kb data. Subsequently, the selected 4Kb data are sensed

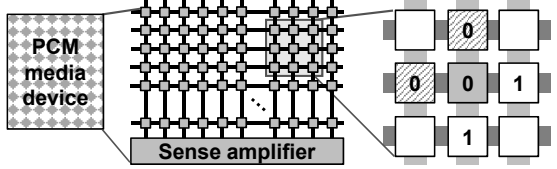


Fig. 1: Illustration of WDE in a cell array. Cells with hatched patterns are disturbed ones that may flip to 1, and darkly shaded cells are aggressors.

by bitline sense amplifiers (BLSA) and transferred through global bitlines (shaded arrow in the figure). Each column multiplexer (MUX) obtains 4Kb data from global bitlines and outputs 8-bit data to global sense amplifiers (S/A) with column address, from which the output procedure implies that eight consecutive bitlines comprise one column. Finally, 8-word data are transferred to the data bus in burst mode if eight data pins per device are assumed, and totally 64B are carried out since eight devices are driven symmetrically by a single command, as shown in Figure 2(b). For a write operation, the data on write drivers (W/D) are written back to the cell array with differential write [68]. In this paper, it is assumed that the columns are well insulated to each other; hence, the neighboring columns do not incur WDEs. Otherwise, more than four read operations are required for each write operation when VnC is adopted, by which the overhead of baseline design is reduced as well. Furthermore, since the material of PCM is organized to be overlapped with a bitline, the WDE mainly occurs on adjacent materials that are patterned on the same bitline [35].

B. Modeling Write Disturbance in PCM

WDE is a hindrance to the popularization of the device, which shifts the resistance of a cell in amorphous state to crystalline state [23], [48], [50], [64]. As shown in Figure 1, WDE occurs on an idle cell adjacent to the cell under a RESET operation [23], [64]. The heat dissipated during a SET operation is nearly half of that during a RESET operation. Therefore, the temperature of an idle cell next to the programmed cell would be higher than those cells under SET, but lower than those cells under RESET. As a consequence, a phase transition may occur on that idle cell. In a word, WDEs likely occur on idle cells having high resistance, where the neighbors are being programmed as 0.

Noticing *when* a WDE occurs is also crucial for modeling a WDE in a simulator. Unlike the probabilistic model that incurs WDE for a specific probability [23], [63], [64], the previous study recently reports that a WDE is incurred by the accumulation of a number of write operations [21]. Specifically, it occurs when a cell is being continuously exposed to a relatively high temperature. Thus, if cells around an idle cell are under RESET for a certain number of times, that idle cell would have a high chance of disturbance [51]. In [51], the authors declare their cell model in amorphous state crystalizes after $1E+09$ times of pulses (50ns for each pulse) on neighbor cells, where each programming is not in the same time frame. Recently, manufacturers specify the limitation number of repetitive writes as 5K-10K [21]. From

this perspective, an on-demand rewrite is required to handle the disturbance-vulnerable pattern (i.e., 1-to-0 flip) **just before** WDE occurs. In this study, it is assumed that the disturbance limitation number is 1K (i.e., WDE occurs when the cell is exposed to 1K number of 1-to-0 flips on neighbors), as reported by [21].

C. Related Works and Motivation

Various studies aimed at reducing WDEs in PCM have been reported. VnC is the most naïve and rigid method to prevent from WDE [64]. It reads two neighbor data before writing data for verification. Subsequently, the data is read again after the data is written, and the correction is performed if WDEs occur. Although it is an effective WDE mitigation method, significant performance overhead is induced by four more read operations for each write operation (including correction). In [64], *lazy correction* is built on top of an error correction pointer (ECP) chip, by which locations of disturbed cells are temporarily stored in the ECP; hence, the correction can be deferred as late as possible until the ECP becomes full within a super-dense PCM module (SD-PCM). However, it requires one additional device which has larger process technology than normal devices.

Since VnC-based approaches incur considerable performance overhead, some methods have been proposed to reduce WDE vulnerable patterns by leveraging data encoding; hence, less or no VnC is required. In [23], *DIN* proposes a codebook that encodes contiguous 0s in a compressed cache line as “01” or “10” patterns; therefore, it may eliminate disturbance-vulnerable patterns as much as possible. However, the encoded data need to be in the range of the length of the cache line (i.e., 512 bits); otherwise, it has to fall back to VnC method, which incurs significant performance degradation. In [17], *MinWD* encodes write-data into three candidates with special shift operations and selects the least aggressive encoding form among candidates. However, the encoding methods generally require to be supported by multi-bit error correction code, which is unaffordable in typical client nodes, unlike server side. In [59], *ADAM* compresses a cache line with the frequent-pattern compression (FPC) and aligns the line to the right and left alternately. Therefore, adjacent cells holding valid data bits are lowered significantly. However, it is still vulnerable to WDEs if the length of the compressed word is longer than 50% of the original data length.

Data caches have been utilized for enhancing throughput of a system; however, it also can be leveraged for reducing WDEs by temporally storing frequently written data into the more reliable volatile region, such as SRAM. In [21], *SIWC* leverages a write cache for absorbing bit flips to reduce WDEs. It utilizes a probabilistic method, coin tossing, to evict data from write cache and insert new data with certain probabilities. Since most of the data that may easily incur WDE would be stored in the write cache, the victims of WDE become safe. However, this method introduces several megabytes of volatile memory to obtain higher hit ratio. Furthermore, even if the write cache is embedded in the memory module,

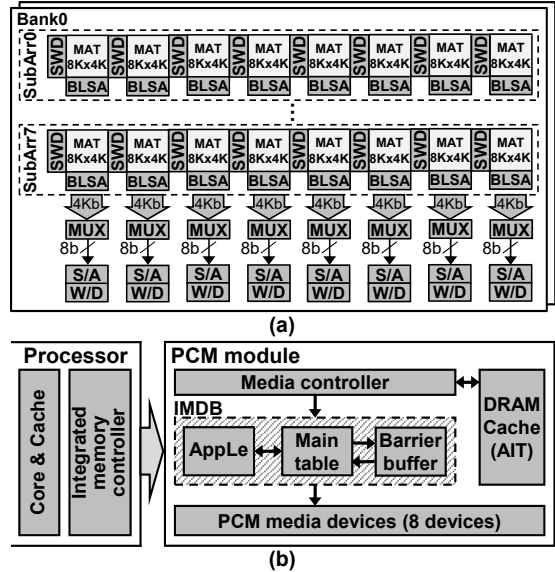


Fig. 2: Overall architecture of the system. (a) detailed view of a PCM device, (b) system layout with IMDB.

the supercapacitor for data flush on a system failure has to be expanded as the volatile region enlarges. Typically, a commercial NVDIMM guarantees that the volatile data must be flushed within 100us [20]. Therefore, the write cache size must be reduced to a more practical value while sufficiently utilizing the disturbance-vulnerable write patterns. Moreover, it is reported that WDEs likely occur when cells are exposed to RESET for specific times [21]; hence, making use of this information is crucial to highly reduce WDEs.

III. IMDB: IN-MODULE DISTURBANCE BARRIER

In this section, an on-demand rewrite method, called IMDB, is proposed by leveraging an SRAM-based table instead of relying on VnC.

A. System overview

Figure 2(b) depicts the overall system layout, where NVM commands are dispatched from the integrated memory controller (iMC) in a processor. For a DIMM-based PCM module, an on-DIMM media controller comprised of read queue and write queue. The scheduler is used for scheduling commands and assigning commands to appropriate banks in the media. A DRAM cache is used for storing address indirection table [20]. The proposed module, IMDB, is located between the media controller and the PCM. It includes the main table, barrier buffer, and a finite state machine controlling entry migration between two tables. Data flip patterns of write commands in this module are managed to trigger rewriting WDE-vulnerable addresses before the occurrences of WDEs, instead of being based on VnC. The introduction of IMDB induces variable latencies during the transaction; however, the iMC in the processor can communicate via DDR-T protocol, which allows variable latencies as in commercial persistent memory products [20].

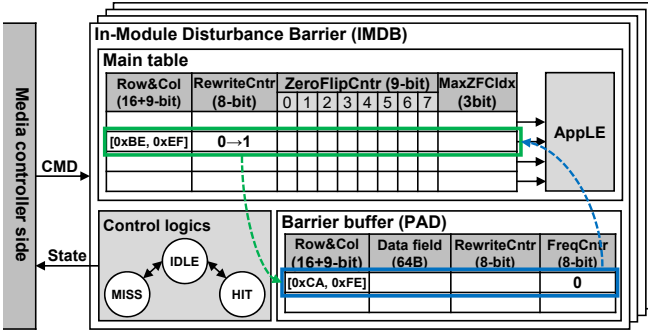


Fig. 3: Architectural design of IMDB. Each IMDB plane is assigned to each PCM bank operation. The entry bounded by the green box indicates the promoted entry from the main table; the entry bounded by the blue box indicates the demoted entry from the barrier buffer.

B. Architectural Design

Figure 3 shows the architecture of the IMDB, which is allocated for every bank; hence, all IMDBs operate concurrently through all banks for a higher command processing throughput and implementation simplicity. An IMDB is comprised of two tables, namely a *main table* and a *barrier buffer*, where the following subsections describe functionalities of each table.

1) Main Table

The main table of IMDB is implemented with a set of SRAMs. Thus, it can only read or write one entry at a time where the content of entry is updated via the control logics. Additionally, data are not stored in the main table for conserving power spent on supercapacitors. Specifically, four major fields are used to estimate the degree of WDE of a written address:

- *Row & Col*: It contains the row and column addresses in a bank that is currently being managed in the main table.
- *ZeroFlipCntr*: Eight sub-counters are in the field, each of which counts the number of bit flips from 1 to 0 and manages each 64-bit data in a 64B cache line.
- *MaxZFCIdx*: It indicates the maximum sub-counter of *ZeroFlipCntr*, which is updated in the control logics after reading an entry. It is used for instantly comparing the maximum value of the *ZeroFlipCntr* with the threshold value for rewrite operations.
- *RewriteCntr*: An 8-bit counter represents the frequency of rewrite operations on the address of *Row & Col*.

Since only one entry can be accessed at a time, resource contention on the IMDB must be considered. This problem is resolved by building a 3-state finite state machine in the control logics, namely IDLE, HIT, and MISS, which represents the availability in the main table. A new command cannot be started by IMDB when the state is not in IDLE, which means that the main table is unavailable. After a command is inserted into one of the IMDB from the media controller, the IMDB operates in two different ways whether the address is found in the table or not:

- If an address is found in the main table, the state transits to HIT. Meanwhile, both newly and previously written data are passed to the control logics, and the number of

1-to-0 bit flips are updated by a dedicated 1-to-0 counter in the control logic (see Section V), where the number is accumulated to the corresponding *ZeroFlipCntr*. When the maximum value of *ZeroFlipCntr* surpasses the pre-defined *threshold*, two rewrites on adjacent wordlines are generated and sent to the write queue in the media controller. Meanwhile, the value of *RewriteCntr* increases. As system reliability is critical, the highest priority is conferred to the rewrite request.

- If an address is not found in the main table, an insertion is required while converting the state to MISS. The probabilistic insertion method is leveraged in this study, where infrequent accesses are filtered out with probability p to reduce evictions from the SRAM. When an insertion is required, the replacement policy defined in this paper determines the victim (explained in Section IV), and thereby the new entry can replace the victim entry.

Additionally, two parameters, the *threshold* of generating a rewrite command and the insertion probability p , must be determined. First, the *threshold* should be decided according to the WDE limitation number, as in Section II-B. Because two wordlines can disturb a wordline, the *threshold* is determined as a half of the WDE limitation number. In this study, *threshold* = 511 since 1K WDE limitation number is assumed; hence, the bit width of each *ZeroFlipCntr* becomes 9. Regarding to the insertion probability p , a large value incurs frequent entry evictions, whereas a small value may skip the rewrite process even after a wordline reaches the WDE limitation. In this paper, p is assumed to be 1/128, since it can capture most of the malicious attacks for all benchmarks, as derived from various experiments.

2) Barrier Buffer

A higher-tier table, the barrier buffer, is leveraged to store the address and the data experienced frequent 1-to-0 bit flips, as presented in Figure 3. For a read request, the barrier buffer is capable of serving it directly to the host. For a write command, if the address hits on the barrier buffer, the data is updated in the barrier buffer directly. Otherwise, the normal operation of the main table is performed if the address hits on the main table, as explained above.

As shown in Figure 3, the entry bounded by green box is frequently exposed to 1-to-0 flips in the main table. Subsequently, it is invalidated and promoted to the barrier buffer when *RewriteCntr* increments (i.e., rewrite occurs in the main table). The barrier buffer inherits the address and *RewriteCntr* information from the main table. If the barrier buffer is not full, the promoted entry can be directly placed into empty place in the barrier buffer. On the contrary, the promoted entry replaces the least frequently used (LFU) entry that is bounded by blue box in the figure; hence, *FreqCntr* is required for the replacement policy, as in practical online detector (PAD) [44]. On the other hand, the data of the LFU entry is sent back to the media controller for writing back the dirty data, and the information of the LFU entry is demoted to the entry of the main table where the promoted entry has been placed.

As a result, the barrier buffer only stores the frequently flipped data; hence, it can further reduce WDEs. Since the barrier buffer can function concurrently with the main table, the latency can be hidden. The sensitivity analysis of the number of entries would be shown in Section VI.

C. Implementation of IMDB and Rebuild of Media Controller

In practice, both the main table and the barrier buffer in the IMDB are implemented as two sets of SRAMs. For the main table, two types of SRAMs are utilized. First of all, a dual-port content-addressable memory-based (CAM) SRAM is allocated as *Row* & *Col* fields for indexing the entries in the table and confirming the existence of the address in the table. On the other hand, a multi-port SRAM, consisting of *ZeroFlipCntr*, *MaxZFCIdx*, and *RewriteCntr*, has one write port for updating content and multiple read ports for obtaining the entry information at once to apply the proposed replacement policy; hence the number of read ports is same as the number of entries in the table. However, the next subsection shows that the number of read ports can be reduced by adopting *AppLE*. For the barrier buffer, a dual-port CAM-based SRAM and a dual-port SRAM are assigned for *Row* & *Col* and *data* & *RewriteCntr* & *FreqCntr*, respectively. The burden of energy consumption is negligible because only a small number of entries in the barrier buffer is enough to provide high WDE mitigation performance, as shown in Section VI-G3. It should be noted that the valid bits are merely implemented as registers for direct probing of status.

The media controller is modified slightly to support the IMDB. First, previously written data must be acquired ahead as well to count bit flips. Thus, a *pre-write read operation* is required to get the previously written data. The controller holds one more data buffer to carry the old data, and an additional bit is required to distinguish the prepared commands from unprepared ones (here called “prepared”). The pre-write read request is generated ahead of the write request. It has a higher priority than write requests but lower priority than normal read requests. Since write requests in the media controller are drained when the write queue becomes full, a long idle time remains between the reading and writing data from/back to the PCM media [64]. In addition, a merge operation of write requests is introduced. It merges the rewrite operation with the existing write requests of the same address. Since a rewrite operation entirely writes all bits of data, excessive rewrites may incur cascaded WDEs on neighbor lines continuously. Therefore, coalescing rewrite requests to existing requests in the queue may further reduce WDEs.

D. Discussion of Applicability

Considering the capacity of SRAM for the proposed method and a write cache-based study, *SIWC*, the latter requires $256 \times 64B = 32KB$ of SRAM for each PCM bank (if 256 addresses are managed). On the other hand, in the proposed method, the main table entry has $25b + 8b + 72b + 3b = 108b$, and the barrier buffer entry has $64B + 25b + 8b + 8b = 553b$ (see Figure 3). Therefore, the proposed method requires $256 \times 108b \approx 3.4KB$ of SRAM on the main table per PCM bank,

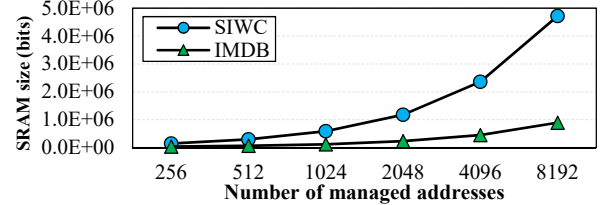


Fig. 4: Required capacity of SRAM with respect to different numbers of managed addresses.

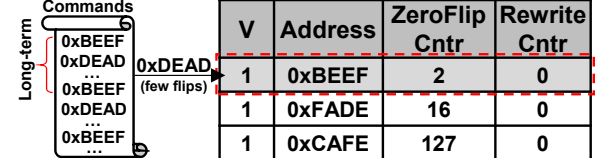


Fig. 5: A toy example showing that the main table is under malicious attack.

and the barrier buffer consumes $8 \times 553b \approx 0.6KB$ of SRAM per PCM bank (see Section VI-E). Consequently, totally $(3.4KB + 0.6KB) \times 4\text{-bank} = 16KB$ of SRAM translates to 2KB per 1GB of PCM. Figure 4 shows the capacity of SRAM with regard to different numbers of managed addresses in SRAM for both *SIWC* and the proposed method. If 256 addresses are managed in an SRAM, the proposed method consumes an SRAM area that is 4 times smaller than that of *SIWC*. In addition, more energy must be stored in the supercapacitor to flush data during system failure. *SIWC* requires approximately 32 times more energy in the supercapacitor compared with the proposed method (i.e., 256-entry/8-entry=32). As the relationship between the energy (*E*) and area (*A*) of a capacitor is $E \propto A$, *SIWC* requires 32 times more area by supercapacitors. Since the write latency of some PCM is 150ns, it requires more than $256 \times 150\text{ns} / 100\text{us} = 38.4\%$ of the constraint (i.e., 100us), as in *SIWC*. Hence, the proposed method is more practical to be adopted in a real system.

IV. REPLACEMENT POLICY OF IMDB

A. Replacement Policy

A replacement (or eviction) policy managing WDEs in a limited table is required, based on the disturbance-vulnerable patterns. The least recently used (LRU) policy is a representative management policy that keeps tracks of the recency of access information in a constrained data structure. However, WDE occurs when a cell is overly flipped; hence, it is necessary to manage the frequency of 1-to-0 flips and select replaced entry according to that information. In summary, a replacement policy that utilizes the knowledge of disturbance-vulnerable pattern in a limited table is desired to evict invulnerable address information. In this study, a replacement policy is defined by exploiting *ZeroFlipCntr* and *RewriteCntr*. The former shows the degree of interference to adjacent wordlines presently, and the latter declares the degree of interference to adjacent wordlines historically, as briefly explained in the previous section.

When the input command demands a new entry in the main table that is fully occupied if the correspondence is not found, the policy is ready to select a victim entry. The minimum

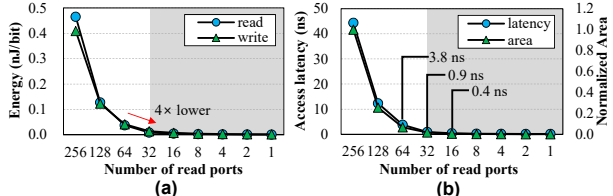


Fig. 6: Energy, latency, and area of a 256-entry SRAM having multiple read ports, which is extracted from CACTI [13]. (a) energy, (b) latency and area.

number of *ZeroFlipCntr* is firstly extracted from the main table as a victim candidate because this is less urgent aggressors presently. However, more than two victim candidates may exist due to the same values of *ZeroFlipCntr*. The aggressiveness of incurring WDEs among can be different according to historical information, *RewriteCntr*. Therefore, the entry holding the minimum number of *RewriteCntr* is finally chosen as the replaced entry.

B. Prior Knowledge

The proposed replacement policy well utilizes the knowledge of the disturbance-vulnerable patterns, namely *ZeroFlipCntr* and *RewriteCntr*; however, the proposed policy ignores the “warm-up” phase of entries in the table. Since the policy prioritizes the present vulnerability (i.e., *ZeroFlipCntr*) to restore urgent data on demand, the recently inserted but insufficiently baked entry can be evicted from the main table easily. Although *RewriteCntr* contains the historical knowledge of WDE, it would not be useful if the corresponding entry is unluckily pushed out from the list by other addresses once it is newly inserted.

As shown in Figure 5, 0xBEEF and 0xFADE are recently inserted entries. In this example, 0xFADE luckily has a larger value of *ZeroFlipCntr* than 0xBEEF and the value does not vary dynamically in run time; hence, a new input address 0xDEAD replaces 0xBEEF according to the policy. However, 0xBEEF tends to incur WDEs frequently with slow and gradual 1-to-0 bit flips, which can be seen as a kind of malicious attack. In a word, since the eviction predicate is no longer the recency as the LRU policy, and a newly inserted entry may have a small value of *ZeroFlipCntr*; hence, these entries would be replaced by new addresses easily without being aware of malicious access under the management of IMDB. Therefore, on the top of the replacement policy, *further knowledge* is required to prevent attacks of such addresses.

To tackle this problem, this paper confers **prior knowledge** that prevents the entry from early eviction. The prior knowledge is merely defined as the number of zeros in each data block; hence, a 0-counter embeds in the control logic of IMDB along with 1-to-0 counter. When an address newly inserted into the main table, the prior knowledge is recorded into *ZeroFlipCntr* as a bias value instead of barely recording the number of 1-to-0 flips in the field. The effectiveness of the proposed method is verified and compared with the case without the method in Section VI-D.

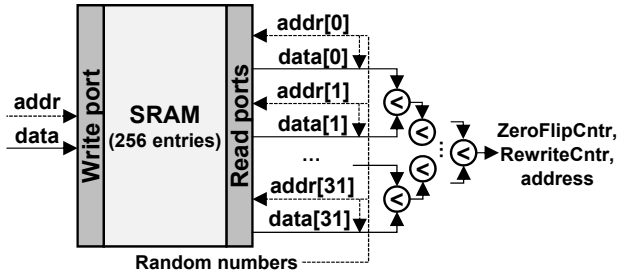


Fig. 7: Implementation of AppLE with 32 read ports.

C. Approximate Lowest Number Estimator

The eviction policy requires a multi-port SRAM and a set of comparators to obtain the victim entry among all entries, where the number of read ports on the SRAM equals the number of entries. However, both the latency, area, and energy becomes larger as the number of read ports increases (see Figure 6). Assuming 256 entries in the main table, the comparator is modeled as tree-structured 255 dual-input comparators to minimize the latency (i.e., 8 cycles). Therefore, 256 read ports are required on the SRAM. Although the multi-port SRAM has been adopted in the previous study for different purpose [31], it is infeasible in the practical design with regard to both latency, area, and energy if there are hundreds of read ports table has hundreds of entries. Figure 6(a) presents energy consumption with regard to the number of read ports on SRAM. The energy consumption drastically decreases when there are 32 read ports. Moreover, Figure 6(b) shows that the latency of SRAM is below 1ns, and the area drastically shrinks on 32 ports. Since the typical I/O clock frequency of DDR4 is above 800MHz [36], the maximum target number of read ports in this paper is set to 32.

In this paper, a comparator structure with an approximate lowest number estimator (AppLE) is introduced to reduce the number of read ports, as shown in Figure 7. It binds a few entries (e.g., 8 entries) as a group, and thereby yielding 32 groups, that is, 32 read ports are required rather than expanding the high-cost 256 read ports by adopting AppLE. A number ranging from 0 to 7 is randomly generated from each group and fed to each address signal of the read port, where the values of *port-index* \times 32 are added to each random number as offsets. Consequently, a comparator module with 5-cycle latency and 31 dual-input sub-comparators can be obtained. This methodology can be regarded as a randomized method, where the group size determines the WDE mitigation performance. The sensitivity analysis between the group size and WDEs is presented in Section VI-E.

V. PUTTING ALL MODULES TOGETHER: CASE STUDIES

In this section, all of the modules discussed in the previous sections are bound as a single module, and a toy example is explained in a step-by-step fashion, as shown in Figure 8. The example assumes that row and column addresses are commonly 8 bits. The target address to incur WDEs on neighbors in this example is assumed as 0xBEEF, where the row address and the column address are 0xBE and 0xEF, respectively. Two bytes of data are carried by a write command, and a single

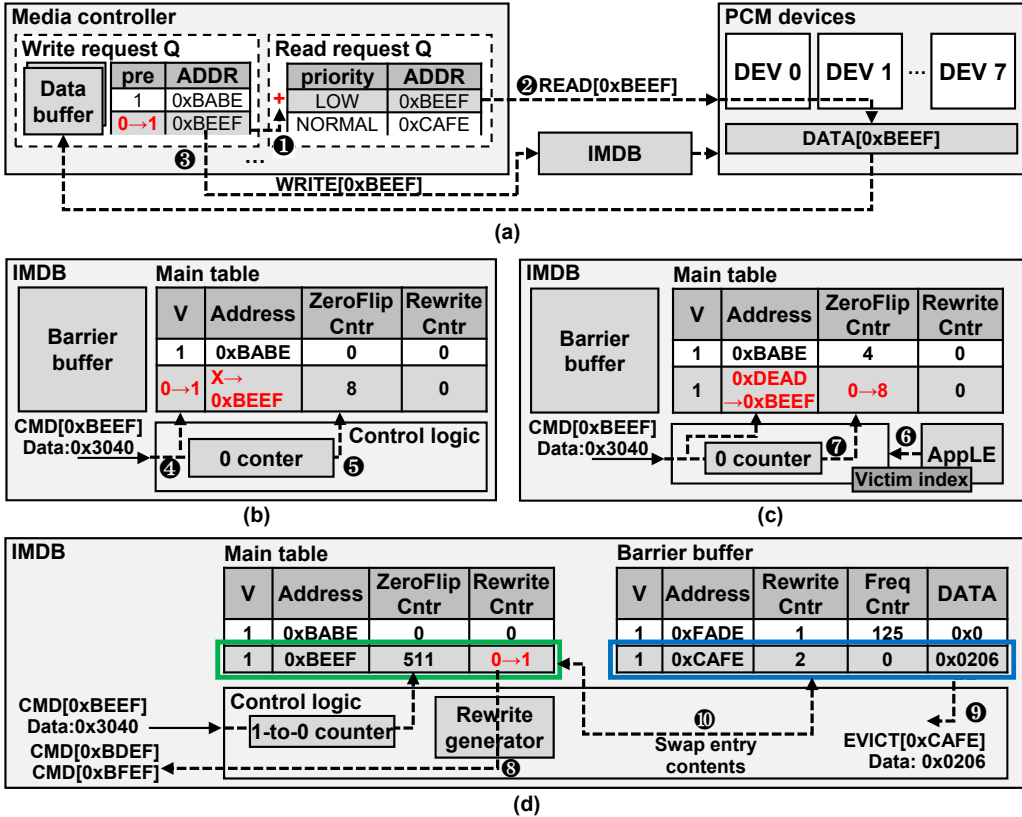


Fig. 8: Operation of IMDB in different cases. (a) data preparation on the media controller, (b) insertion on the non-empty main table, (c) replacement on the full main table, (d) entry promotion and demotion.

ZeroFlipCntr manages all data. Both the main table and the barrier buffer consist of four entries.

Data preparation. The media controller receives a write command from the processor iMC, and it is held to read the data already stored in the PCM device to prepare to count 1-to-0 flips in the IMDB (1). Once the old data arrives through the read phase of the media controller (2), the command along with new and old data are issued to the IMDB (3).

Filling the main table. As the command in the previous step arrives, the control logic decomposes the command address into row and column addresses to confirm whether it is a hit or a miss on the tables. In this case, misses occur both on the barrier buffer and the main table; however, the main table has a vacant space for the input command, which means that the command information can be stored in the table directly by merely validating entry instead of replacing it (4). As discussed in Section IV-C, the number of zeros in the write data is recorded in *ZeroFlipCntr* to prevent early eviction from the table without a “warm-up” period. If subsequent commands access the same address, 1-to-0 flip counts are calculated and added to the current *ZeroFlipCntr* (5).

Replacement on the main table. When the main table becomes full, and there is no entry available for the next input command, a victim candidate should be selected to make room for the input command 0xBEEF. As shown in the figure, the entry storing the information of 0xDEAD has the lowest number of *ZeroFlipCntr* among all entries, as computed from AppLE (6); hence, all information of 0xDEAD is replaced

by 0xBEEF at once (7).

Entry promotion and demotion. When repetitive writes to 0xBEEF with a frequent number of 1-to-0 flips cause *ZeroFlipCntr* to reach the threshold value (see Section III-B1), rewrite commands on neighboring lines (i.e., 0xBDEF and 0xBFEF) are generated and sent back to the media controller (8). Meanwhile, the barrier buffer selects a victim entry and demotes it to the main table. Furthermore, the eviction command is generated based on the victim entry and sent back to the media controller (9). After both the demoting entry and the entry incurring the rewrite operation (i.e., promoting entry) are read out from the table, they are interchangeably stored in the main table and the barrier buffer. Specifically, the promoting entry is stored with the write-data to prevent a WDE before it occurs (10).

VI. EVALUATIONS

A. Configurations

As shown in Table I, the PCM system is built upon an NVM simulator, *NVMain* [42]. The read latency is set to 100ns, and the write latencies of SET and RESET are set to 150ns and 100ns, respectively, with the differential write support [68]. The *baseline* in this paper does not adopt any WDE mitigation method. The energy per access on PCM and CAM-based SRAM is obtained from NVSim and CACTI, respectively, both of which are configured with 22nm technology [7], [13]. It should be noted that CAM-based SRAM is configured as a fully associative cache.

Table II shows the workloads and associated misses per thousand instructions (MPKI) on the last-level cache. Normal workloads from SPEC CPU 2006 consisting of both high and low MPKI are evaluated. Furthermore, persistent data structures performing random insertions and deletions throughout 128 copies are implemented. This paper synthesizes these data structures to create four persistent workloads (prefixed as “pmix”) to simulate realistic in-memory database workloads because persistent workloads would generally be executed under an NVM-based main memory system [6], [22], [24]. Trace-based simulation is conducted to reduce the simulation time. The trace files of the discussed workloads are extracted from the processor simulator *gem5*, as shown in Table I [2].

The proposed method is compared with three representative studies, *lazy correction*, *ADAM* and *SIWC*, as explained in Section II. In following subsections, *SIWC-size* indicates that the number of SRAM bytes for *SIWC* is identical to that of the proposed method, and *SIWC-entry* holds entries in an amount equal to that of the proposed method. Finally, *lazy correction* indicates that ten errors are held in ECP devices.

B. Architectural Exploration

Design parameters, specifically the number of entries in the main table (N_{mt}), the number of entries in the barrier buffer (N_b), and the number of read ports (i.e., group size) dedicated to AppLE (N_g), are crucial when seeking to realize a cost-effective architecture for the proposed method. The trade-off function of the proposed method can be defined using the following equation, where W , A , and S are the number of WDEs, the area, and the speedup, respectively:

$$T = W(N_{mt}, N_b, N_g) + A(N_{mt}, N_b, N_g) + S^{-1}(N_b, N_g) \quad (1)$$

As explained in the previous section, the area consumed by SRAM can shrink noticeably from $N_g = 32$ (see Figure 6), also making the measurement negligible if $N_g < 32$, as compared to PCM. Moreover, 32 is defined as the maximum number of entries in the barrier buffer to guarantee that no more than 10% of the flush time (i.e., 100us) is consumed when using the proposed method (see calculation in Section III-D). As a result, the equation (1) can be simplified, as follows:

TABLE I: Simulation configurations

Simulator	Device	Description
gem5	Cores	Out-of-order, 4-core, 2GHz
	L1 cache	I-cache: 2-way set associative, D-cache: 4-way set associative, each has a capacity of 64KB.
	L2 cache	Shared last-level cache. 16-way set associative, 1MB.
NVMMain	Media controller	Separated write queue and read queue (64-entry), FR-FCFS.
	PCM	Differential write supported Read: 100ns RESET: 100ns, SET: 150ns Write disturbance limitation: 1K Size: 8GB (2-rank, 2-bank/rank)

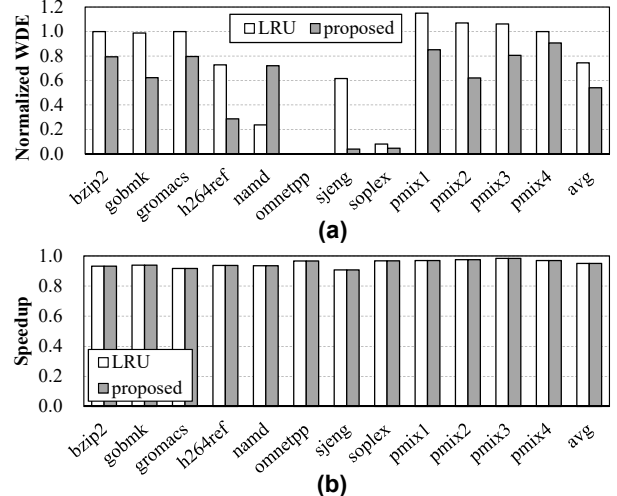


Fig. 9: Performance according to different replacement policies.
(a) normalized WDE, (b) speedup.

$$T = W(N_{mt}, N_b, N_g) + A(N_{mt}, N_b) + S^{-1}(N_b, N_g), \quad (2)$$

where $N_g \leq 32, N_b \leq 64$

According to the equation, this section evaluates the effectiveness of the prior knowledge and determines the appropriate size of the main table (N_{mt}) as well. Subsequently, sensitivity analyses with respect to the number of entries in the barrier buffer (N_b) and the group size for AppLE (N_g) are conducted to determine the cost-effective parameters. Finally, these parameters are applied and compared with those in previous studies to show the performance of the proposed method.

C. Effectiveness of the Replacement Policy

Before exploring the proposed architecture, verifying the effectiveness of the proposed policy is necessary. Figure 9 shows the WDEs with different replacement policies when there are 16 entries in the main table. It should be noted that barrier buffers are not applied for a simpler comparison. As shown in Figure 9(a), the least recently used (LRU) scheme is applied as the policy in the main table, which yields a normalized WDE value of 0.74 on average. In contrast, the proposed policy shows a normalized WDE of 0.54, indicating a 27% more reliable system compared to the traditional replacement policy. Although LRU yields fewer WDEs in

TABLE II: Information of workloads

Workloads	Description	MPKI
SPEC::bzip2	General compression	11.98
SPEC::sjeng	Artificial intelligence (chess)	0.89
SPEC::h264ref	Video compression	1.65
SPEC::gromacs	Biochemistry	5.49
SPEC::gobmk	Artificial intelligence (go)	6.65
SPEC::namd	Biology	1.09
SPEC::omnetpp	Discrete event simulation program	6.99
SPEC::soplex	Linear programming optimization	21.31
pmix1	Queue, Hashmap, B-tree, SkipList	10.24
pmix2	Queue, B-tree, RB-tree, SkipList	11.10
pmix3	Hashmap, RB-tree, Queue, SkipList	8.95
pmix4	RB-tree, Hashmap, B-tree, SkipList	10.12

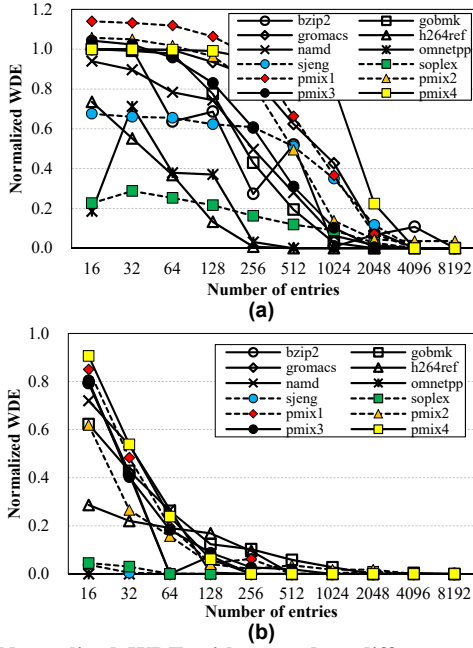


Fig. 10: Normalized WDE with regard to different numbers of entries in the main table. (a) without prior knowledge, (b) with prior knowledge.

applications with extremely high rates of locality (e.g., *namd*) [25], most general applications yield far fewer WDEs.

Figure 9(b) presents the speedup, which is defined as the execution time of the baseline over the execution time of the objective method [64]. Both methods provide similar performance outcomes, where the proposed method shows 0.002% lower performance than the LRU policy. From this perspective, the proposed replacement policy efficiently rewrites data vulnerable to WDEs and thereby yields far fewer WDEs without compromising high-performance computing.

D. Effectiveness of Prior Knowledge and Entries

Figure 10 shows the normalized WDE according to different numbers of entries in the main table. As illustrated in both figures, WDEs decrease as the number of entries increases. When a relatively small table is adopted, the number of WDEs exceeds that in the baseline due to the frequent evictions of newly inserted entries in a full table. Moreover, WDEs decrease sharply from 2048 entries without prior knowledge, as shown in Figure 10(a).

On the other hand, the prior knowledge method with 256 entries provides a result equivalent to the method without prior knowledge and with 2048 entries, as shown in Figure 10(b). In other words, the proposed method yields an eightfold increase in the efficiency of the WDE mitigation performance.

Figure 11 presents the average normalized WDE and the capacity required for the main table. As shown in the figure, the normalized WDE is 95% lower than the case without prior knowledge at 256 entries. Furthermore, the capacity of the main table significantly increases from 512 entries; hence, 256 entries can be selected as an appropriate number of entries in the main table considering the trade-off between the performance and the area. In summary, from this subsection,

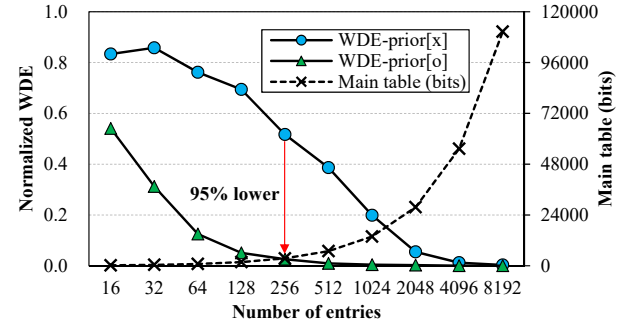


Fig. 11: Average normalized WDE and SRAM capacity regarding different numbers of entries in the main table.

the number of entries in the main table is fixed at $N_{mt} = 256$.

E. Effectiveness of the Barrier Buffer

The barrier buffer, a small table containing data frequently flipped from 1 to 0, is expected to yield fewer WDEs. Figure 12 shows the performance with different numbers of entries in the barrier buffer. For clarity, the results of both figures in Figure 12 are normalized to the case when the main table consists of 256 entries and is supported by prior knowledge (called **temporal base condition** in this subsection only). Moreover, the figures show WDEs of benchmarks still containing errors under the temporal base condition, whereas other benchmarks maintain their free-WDE status.

In Figure 12(a), most of the benchmarks yield significantly lower numbers of WDEs with the barrier buffer from four entries. However, for *gobmk*, WDEs decrease when the barrier buffer containing 64 entries is applied. This occurs because some addresses have extremely long-period write-access patterns, which are hardly a concern of the proposed replacement policy regardless of whether or not the barrier buffer is applied. However, under the temporal base condition, WDEs are reduced by 90% relative to the baseline. Furthermore, in the following sub-section, the slightly randomized method, AppLE, is shown to be able to mitigate this problem.

Figure 12(b) shows the average normalized WDE and speedup values of the benchmarks mentioned above. The figures show that the speedup does not increase markedly for all ranges; hence, S^{-1} is referred to as a constant in the equation (2). Furthermore, the capacity of the barrier buffer is at least three times as small as the main table for $N_b \leq 16$ (see the number of bits for the entries in the tables in Section III-D), which makes the capacity of the barrier buffer negligible compared to the main table. Therefore, analyzing

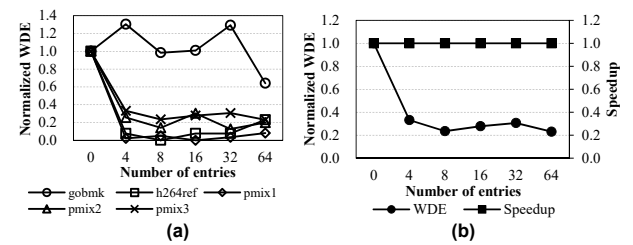


Fig. 12: Performance with different numbers of entries in the barrier buffer normalized to the temporal base condition. (a) normalized WDE, (b) average of normalized WDE and speedup.

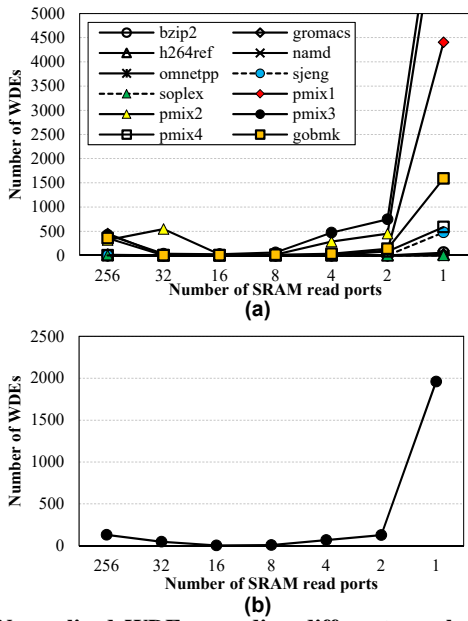


Fig. 13: Normalized WDE according different numbers of read ports for AppLE. (a) normalized WDE of benchmarks, (b) average normalized WDE.

W in equation (2) is sufficient to obtain a cost-effective architecture, and $N_b = 8$ is selected as the trade-off point because the normalized WDE decreases stably from the point of 8, as shown in Figure 12(b).

F. Sensitivity Analysis on AppLE

AppLE is proposed to mainly reduce the number of read ports on SRAM for the replacement policy. Therefore, a sensitivity analysis with respect to the group size, which is regarded as the number of read ports on SRAM, is required because the proposed method is a randomized approach. For a straightforward analysis, the barrier buffer is not applied in this evaluation. Furthermore, the group size begins from 32 due to the feasibility of this value in a practical system (see Section IV-C). Figure 13(a) presents the absolute number of WDEs with different numbers of read ports. Here, 256 read ports means that AppLE is not applied to the system. As presented in the figure, the number of WDEs stabilizes with fewer read ports for most of the benchmarks. In particular, the *gobmk* benchmark, which involves long-period write-access patterns, presents fewer WDEs on fewer number of read ports because it prevents such “tricky addresses” from being evicted from the table by applying the randomized method. However, the WDEs increase significantly from two read ports, as shown in Figure 13(b). For the *fully randomized replacement policy*, i.e., one read port, the number of WDEs is 15 times higher than the case without AppLE, indicating that the fully randomized replacement policy is less reliable than the proposed policy.

Figure 14 presents the energy consumption and speed performance with different numbers of read ports. As shown in Figure 14(a), the speed performance does not vary much according to the number of ports. Therefore, the latency consumed by multiple stages of sub-comparators has nearly no effect on the performance. Additionally, Figure 14(b) shows

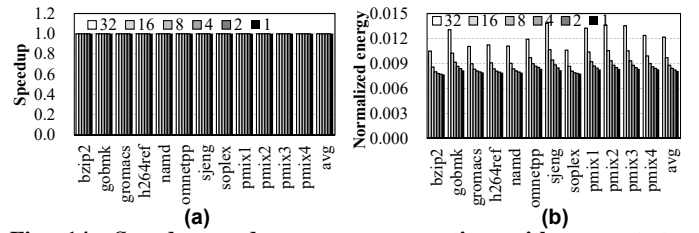


Fig. 14: Speedup and energy consumption with respect to different numbers of read ports for AppLE. (a) speedup, (b) normalized energy.

that the energy consumption on SRAM gradually decreases as the number of read ports shrinks. The energy is decreased by 20%, 10%, and 6% when the read ports are decreased from 32 to 16, from 16 to 8, and from 8 to 4, respectively. From this perspective, $N_g = 4$ or $N_g = 8$ can be an appropriate design parameter for AppLE in this study.

G. Comparison with Other Studies

As discussed in the previous subsections, the group size for AppLE and numbers of entries in the main table and the barrier buffer are suitably determined considering the trade-off analyses. In this section, the proposed method is compared with previous representative studies. The cost-effective architecture of the proposed method consisting of 256 entries in the main table, eight entries in the barrier buffer, and with a group size of eight is denoted as IMDB(e256b8g8), and the group size of four is denoted as IMDB(e256b8g4), which is associated with a more aggressive reduction of the number of read ports on SRAM.

1) Write Disturbance Errors

Figure 15 shows the normalized WDEs for each error mitigation methodology. *SIWC-size* presents the highest normalized WDE value, 0.7276, for all methods. This occurs because *SIWC* is a cache-based approach that strongly depends on the number of entries; hence, the worst WDE mitigation performance is presented when the SRAM capacity of *SIWC* is identical to that of the proposed method. In contrast, the normalized WDE value is reduced to 0.0885 (i.e., an 87.84% reduction compared to *SIWC-size*) when *SIWC* manages the same number entries used in the proposed method. However, it consumes 512b/108b=4.74 times more capacity on SRAM. For *ADAM*, it can reduce WDEs markedly by compressing data to lower the number of vulnerable bits; nonetheless, it is effective only if the compression ratio exceeds 0.5; hence, it shows inferior performance, 0.5341 on average. Subsequently, *lazy correction* yields a normalized WDE value as low as 0.1925, as it is a VnC-based approach and thereby removes errors effectively by sacrificing the speed (see the next subsection).

On the other hand, IMDB(e256b8g4) shows that WDEs are significantly reduced to 2.08E-3. Specifically, there are 256 \times , 93 \times , and 43 \times fewer WDEs compared to those by *ADAM*, *lazy correction*, and *SIWC-entry*, respectively. Furthermore, the cost-effective architecture, i.e., IMDB (e256b8g8), presents 84.04% fewer WDEs than IMDB (e256b8g4). It yields 1218 \times , 439 \times , 202 \times better WDE mitigation performance than *ADAM*, *lazy correction*, and *SIWC-entry*, respectively.

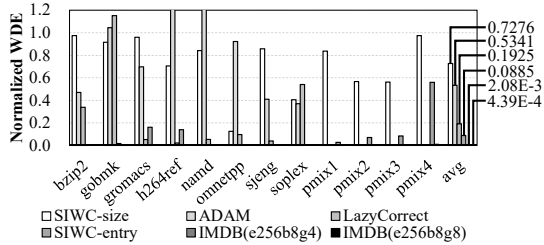


Fig. 15: Normalized WDEs according to different schemes.

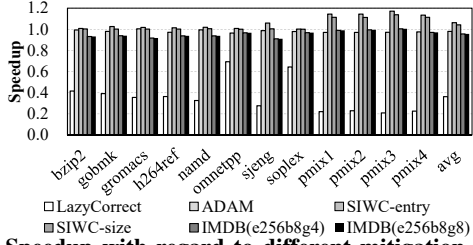


Fig. 16: Speedup with regard to different mitigation schemes.

2) Speedup

Figure 16 presents the speedup of each method compared to the baseline. The figure shows that the speedup of *lazy correction* is $0.36\times$, the lowest among all methods because each write incurs at least four read operations, despite the fact that using this method reduces the number of corrections by leveraging a high-cost ECP device. Although the proposed method must rewrite two instances of adjacent data, the rewrite operation is performed in an on-demand fashion instead of incurring four read operations per write operation, as VnC does. Therefore, the proposed method outperforms *lazy correction*.

In contrast, the speedup of *ADAM* is degraded by 2% compared to the baseline method due to the overhead of FPC. For *SIWC-entry* and *SIWC-size*, the write cache can directly serve data to the processor; hence, it provides the highest speedup of up to $1.06\times$ and $1.04\times$, respectively. The objective of this study is to provide a highly reliable system with negligible performance loss as compared to the baseline that does not adopt any error mitigation method. In this regard, the proposed method yields approximately 4% speed degradation on average, which is slightly lower than the baseline due to the pre-write read operations. Moreover, there is a performance difference of only 0.3% between IMDB (e256b8g4) and IMDB (e256b8g8), which implies that the number of stages on the sub-comparators of AppLE does not influence the speed performance significantly. Meanwhile, there are far fewer WDEs compared to those in previous methods. Although *SIWC-entry* shows a slightly higher speedup, the WDE mitigation performance is much worse than that by the proposed method, resulting in a system with low reliability, as discussed in the previous subsection. As a result, these results imply that the proposed method is suited for highly reliable systems capable of supporting high-performance computing.

3) Energy consumption

Figure 17 presents the normalized energy in the system (i.e., PCM+SRAM). *lazy correction* consumes $2.18\times$ more energy in comparison with the baseline due to redundant operations incurred by VnC. This is 45.87% more energy consumption

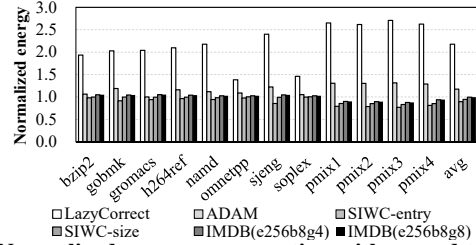


Fig. 17: Normalized energy consumption with regard to different WDE mitigation methods.

than *ADAM*, which is $1.18\times$ higher than the baseline. Despite the fact that it perfectly eliminates WDEs, *lazy correction* performs much slower and uses more operations than the methods without VnC and consequently, it consumes much more energy than the other methods. Meanwhile, the write cache of *SIWC-size* absorbs write operations on highly accessed addresses because persistent workloads have relatively high locality rates caused by cache line flush instructions, which in turn reduces the write energy consumption. Thus, it consumes 5% less energy compared to the baseline. Furthermore, the energy can be lowered to 10.5% with a larger number of entries, as declared by *SIWC-entry*; however, the WDE mitigation performance is not excellent as shown in Figure 15.

The proposed method consumes more energy than *SIWC*. Although IMDB (e256b8g8) presents 9% higher energy consumption compared to *SIWC-entry*, this outcome is still 0.59% lower than the baseline owing to the on-demand rewrite operation and the “tiny” barrier buffer (i.e., normalized energy is 0.9941). Furthermore, compared with the VnC-based approach, *lazy correction*, the proposed method nearly eliminates all errors while consuming 54.4% less energy. These outcomes demonstrate that the proposed method requires only a tiny area without sacrificing either speed or energy efficiency.

VII. CONCLUSION

This study proposes an on-demand table-based method reducing WDEs within a PCM module. The proposed method leverages SRAM tables to manage variations of write data, by which highly vulnerable addresses are rewritten. It declares that table-based method requires a dedicated replacement policy, and prior knowledge of 0s in write data can enhance the WDE mitigation performance. Subsequently, AppLE efficiently downsizes the number of read ports on SRAMs that are incurred by the proposed policy to reduce the both area and energy overhead incurred by the overloaded multi-port SRAMs. It also demonstrates that the LRU and the fully randomized replacement policy are less reliable than the proposed method. On the other hand, a tiny amount of SRAM absorbs further bit flips, allowing the offloading of the supercapacitor burden required on system failures. Consequently, several rigorous sensitivity analyses concerning design parameters are conducted to obtain a cost-effective architecture. The analysis shows that the proposed work can reduce WDEs by $1218\times$, $439\times$, and $202\times$ compared to *ADAM*, *lazy correction*, and *SIWC-entry*, respectively, while maintaining the operation speed and energy consumption that

are almost similar to those of the baseline.

REFERENCES

[1] M. Awasthi, M. Shevgoor, K. Sudan, B. Rajendran, R. Balasubramonian, and V. Srinivasan, "Efficient scrub mechanisms for error-prone emerging memories," in *Proceedings of the 18th International Symposium on High-Performance Computer Architecture (HPCA)*, 2012, pp. 1–12.

[2] N. Binkert, B. Beckmann, G. Black, S. K. Reinhardt, A. Saidi, A. Basu, J. Hestness, D. R. Hower, T. Krishna, S. Sardashti, R. Sen, K. Sewell, M. Shoaib, N. Vaish, M. D. Hill, and D. A. Wood, "The gem5 simulator," *SIGARCH Comput. Archit. News*, vol. 39, no. 2, p. 1–7, Aug. 2011. [Online]. Available: <https://doi.org/10.1145/2024716.2024718>

[3] N. Castellani, G. Navarro, V. Sousa, P. Zuliani, R. Annunziata, M. Borghi, L. Perniola, and G. Reimbold, "Comparative analysis of program/read disturb robustness for gesbte-based phase-change memory devices," in *IEEE 8th International Memory Workshop (IMW)*, 2016, pp. 1–4.

[4] S. Chen, P. B. Gibbons, and S. Nath, "Rethinking database algorithms for phase change memory," 04 2011, pp. 21–31.

[5] S. Cho and H. Lee, "Flip-n-write: A simple deterministic technique to improve pram write performance, energy and endurance," in *Proceedings of the 42nd Annual International Symposium on Microarchitecture (MICRO)*, Dec 2009, pp. 347–357.

[6] J. Coburn, A. M. Caulfield, L. M. G. A. Akel, R. J. R. K. Gupta, and S. Swanson, "Nv-heaps: making persistent objects fast and safe with next-generation, non-volatile memories," in *Proceedings of the 16th International Conference on Architectural Support for Programming Languages and Operating Systems (ASPLOS)*, 2011, pp. 105–118.

[7] X. Dong, C. Xu, Y. Xie, and N. P. Jouppi, "Nvsim: A circuit-level performance, energy, and area model for emerging nonvolatile memory," *IEEE Transactions on Computer-Aided Design of Integrated Circuits and Systems*, pp. 994–1007, July 2012.

[8] S. R. Dulloor, S. Kumar, A. Keshavamurthy, P. Lantz, D. Reddy, R. Sankaran, and J. Jackson, "System software for persistent memory," in *Proceedings of the 9th European Conference on Computer Systems (EuroSys)*, 2014, pp. 15:1–15:15.

[9] J. Fan, S. Jiang, J. Shu, Y. Zhang, and W. Zhen, "Aegis: Partitioning data block for efficient recovery of stuck-at-faults in phase change memory," in *Proceedings of the 46th Annual International Symposium on Microarchitecture (MICRO)*, 2013, pp. 433–444.

[10] A. P. Ferreira, M. Zhou, S. Bock, B. Childers, R. Melhem, and D. Mossé, "Increasing pcm main memory lifetime," in *Proceedings of the Conference on Design, Automation and Test in Europe (DATE)*, 2010, pp. 914–919.

[11] J. Guerra, L. Mármol, D. Campello, C. Crespo, R. Rangaswami, and J. Wei, "Software persistent memory," in *2012 USENIX Annual Technical Conference*, 2012, pp. 22–29.

[12] F. T. Hady, A. Foong, B. Veal, and D. Williams, "Platform storage performance with 3d xpoint technology," *Proceedings of the IEEE*, vol. 105, no. 9, pp. 1822–1833, 2017.

[13] Hewlett Packard Lab. Cacti 6.5. [Online]. Available: <https://www.hpl.hp.com/research/cacti/>

[14] F. Huang, D. Feng, W. Xia, W. Zhou, Y. Zhang, M. Fu, C. Jiang, and Y. Zhou, "Security rbsg: Protecting phase change memory with security-level adjustable dynamic mapping," in *Proceedings of the 30th IEEE International Parallel and Distributed Processing Symposium (IPDPS)*, 2016, pp. 1081–1090.

[15] J. Huang, K. Schwan, and M. K. Qureshi, "Nvram-aware logging in transaction systems," *Proceedings of VLDB Endowment*, vol. 8, pp. 389–400, 2014.

[16] M. Imran, T. Kwon, J. M. You, and J. Yang, "Flipey: Efficient pattern redistribution for enhancing mlc pcm reliability and storage density," in *2019 IEEE/ACM International Conference on Computer-Aided Design (ICCAD)*, 2019, pp. 1–7.

[17] M. Imran and J.-S. Y. T. Kwon, "Effective write disturbance mitigation encoding scheme for high-density pem," in *2020 Design, Automation Test in Europe Conference Exhibition (DATE)*, 2020.

[18] Intel. (2019) Intel memory drive technology set up and configuration guide. [Online]. Available: <https://www.intel.com/content/dam/support/us/en/documents/memory-and-storage/intel-mdt-setup-guide.pdf>

[19] E. Ipek, J. Condit, E. B. Nightingale, D. Burger, and T. Moscibroda, "Dynamically replicated memory: Building reliable systems from nanoscale resistive memories," in *Proceedings of the 15th International Conference on Architectural Support for Programming Languages and Operating Systems*, ser. ASPLOS XV. New York, NY, USA: Association for Computing Machinery, 2010, p. 3–14. [Online]. Available: <https://doi.org/10.1145/1736020.1736023>

[20] J. Izraelevitz, J. Yang, L. Zhang, J. Kim, X. Liu, A. Memaripour, Y. J. Soh, Z. Wang, Y. Xu, S. R. Dulloor, J. Zhao, and S. Swanson. (2019) Basic performance measurements of the intel optane DC persistent memory module. [Online]. Available: <http://arxiv.org/abs/1903.05714>

[21] J. Jang, W. Shin, J. Choi, Y. Kim, and L. Kim, "Sparse-insertion write cache to mitigate write disturbance errors in phase change memory," *IEEE Transactions on Computers*, vol. 68, no. 5, pp. 752–764, May 2019.

[22] J. Jeong, C. H. Park, J. Huh, and S. Maeng, "Efficient hardware-assisted logging with asynchronous and direct-update for persistent memory," in *Proceedings of the 51st International Symposium on Microarchitecture (MICRO)*, Oct 2018, pp. 520–532.

[23] L. Jiang, Y. Zhang, and J. Yang, "Mitigating write disturbance in super-dense phase change memories," in *2014 44th Annual IEEE/IFIP International Conference on Dependable Systems and Networks*, June 2014, pp. 216–227.

[24] A. Joshi, V. Nagarajan, S. Viglas, and M. Cintra, "Atom: Atomic durability in non-volatile memory through hardware logging," in *Proceedings of the 23rd International Symposium on High Performance Computer Architecture (HPCA)*, 2017, pp. 361–372.

[25] A. Kejariwal, A. V. Veidenbaum, A. Nicolau, X. Tian, M. Girkar, H. Saito, and U. Banerjee, "Comparative architectural characterization of spec cpu2000 and cpu2006 benchmarks on the intel® core™ 2 duo processor," in *2008 International Conference on Embedded Computer Systems: Architectures, Modeling, and Simulation*, 2008, pp. 132–141.

[26] H. Kim, S. Seshadri, C. L. Dickey, and L. Chiu, "Evaluating phase change memory for enterprise storage systems: A study of caching and tiering approaches," in *12th USENIX Conference on File and Storage Technologies (FAST 14)*. Santa Clara, CA: USENIX Association, Feb. 2014, pp. 33–45. [Online]. Available: <https://www.usenix.org/conference/fast14/technical-sessions/presentation/kim>

[27] M. Kim, J. Choi, H. Kim, and H. Lee, "An effective dram address remapping for mitigating rowhammer errors," *IEEE Transactions on Computers*, vol. 68, no. 10, pp. 1428–1441, 2019.

[28] Y. Kim, R. Daly, J. Kim, C. Fallin, J. H. Lee, D. Lee, C. Wilkerson, K. Lai, and O. Mutlu, "Flipping bits in memory without accessing them: An experimental study of dram disturbance errors," in *Proceedings of the 41st International Symposium on Computer Architecture (ISCA)*, 2014, pp. 361–372.

[29] Y. Kim, S. Yoo, and S. Lee, "Write performance improvement by hiding r drift latency in phase-change ram," in *DAC Design Automation Conference 2012*, 2012, pp. 897–906.

[30] E. Kultursay, M. Kandemir, A. Sivasubramaniam, and O. Mutlu, "Evaluating srtt-ram as an energy-efficient main memory alternative," in *IEEE International Symposium on Performance Analysis of Systems and Software (ISPASS)*, 2013, pp. 256–267.

[31] C.-H. Lai, J. Zhao, and C.-L. Yang, "Leave the cache hierarchy operation as it is: A new persistent memory accelerating approach," in *Proceedings of the 54th Annual Design Automation Conference (DAC)*, ser. DAC '17. New York, NY, USA: ACM, 2017, pp. 5:1–5:6. [Online]. Available: <https://doi.acm.org/10.1145/3061639.3062272>

[32] B. C. Lee, E. Ipek, O. Mutlu, and D. Burger, "Architecting phase change memory as a scalable dram alternative," in *Proceedings of the 36th Annual International Symposium on Computer Architecture (ISCA)*, 2009, pp. 2–13.

[33] E. Lee, I. Kang, S. Lee, G. E. Suh, and J. H. Ahn, "Twice: Preventing row-hammering by exploiting time window counters," in *Proceedings of the 46th International Symposium on Computer Architecture (ISCA)*. New York, NY, USA: Association for Computing Machinery, 2019, pp. 385–396. [Online]. Available: <https://doi.org/10.1145/3307650.3322232>

[34] H. Lee, M. Kim, H. Kim, H. Lee, and H. Lee, "Integration and boost of a read-modify-write module in phase change memory system," *IEEE Transactions on Computers*, vol. 68, no. 12, pp. 1772–1784, 2019.

[35] S. H. Lee, "Method of driving phase change memory device capable of reducing heat disturbance," US Patent 0204 664, 2014.

[36] Mentor-Graphics. (2013) Ddr4 and lpddr4 - broad design verification and challenges. [Online]. Available: <https://www.mentor.com/pcb/multimedia/player/ddr4-and-lpddr4-board-design-verification-and-challenges-356bbc16-6195-4d78-ba85-5496362bec44>

[37] V. Mironov, A. Kudryavtsev, Y. Alexeev, A. Moskovsky, I. Kulikov, and I. Chernykh, "Evaluation of intel memory drive technology performance for scientific applications," in *Proceedings of the Workshop on Memory Centric High Performance Computing*, ser. MCHPC'18. New York, NY, USA: Association for Computing Machinery, 2018, p. 14–21. [Online]. Available: <https://doi.org/10.1145/3286475.3286479>

[38] O. Mutlu and J. S. Kim, "Rowhammer: A retrospective," 2019.

[39] P. J. Nair, C. Chou, B. Rajendran, and M. K. Qureshi, "Reducing read latency of phase change memory via early read and turbo read," in *Proceedings of the 21st International Symposium on High-Performance Computer Architecture (HPCA)*, 2015, pp. 309–319.

[40] O. Patil, L. Ionkov, J. Lee, F. Mueller, and M. Lang, "Performance characterization of a dram-nvm hybrid memory architecture for hpc applications using intel optane dc persistent memory modules," in *Proceedings of the International Symposium on Memory Systems*, ser. MEMSYS '19. New York, NY, USA: Association for Computing Machinery, 2019, p. 288–303. [Online]. Available: <https://doi.org/10.1145/3357526.3357541>

[41] I. B. Peng, M. B. Gokhale, and E. W. Green, "System evaluation of the intel optane byte-addressable nvm," in *Proceedings of the International Symposium on Memory Systems*, ser. MEMSYS '19. New York, NY, USA: Association for Computing Machinery, 2019, p. 304–315. [Online]. Available: <https://doi.org/10.1145/3357526.3357568>

[42] M. Poremba, T. Zhang, and Y. Xie, "Nvmain 2.0: A user-friendly memory simulator to model (non-)volatile memory systems," *IEEE Computer Architecture Letters*, vol. 14, no. 2, pp. 140–143, 2015.

[43] M. K. Qureshi, "Pay-as-you-go: Low-overhead hard-error correction for phase change memories," in *2011 44th Annual IEEE/ACM International Symposium on Microarchitecture (MICRO)*, 2011, pp. 318–328.

[44] M. K. Qureshi, A. Seznec, L. A. Lastras, and M. M. Franceschini, "Practical and secure pcm systems by online detection of malicious write streams," in *Proceedings of the 17th International Symposium on High-Performance Computer Architecture (HPCA)*, Feb 2011, pp. 478–489.

[45] M. K. Qureshi, V. Srinivasan, and J. A. Rivers, "Scalable high performance main memory system using phase-change memory technology," in *Proceedings of the 36th annual international symposium on Computer architecture (ISCA)*, 2009, pp. 24–33.

[46] M. K. Qureshi, J. Karidis, M. Franceschini, V. Srinivasan, L. Lastras, and B. Abali, "Enhancing lifetime and security of pcm-based main memory with start-gap wear leveling," in *Proceedings of the 42nd Annual International Symposium on Microarchitecture (MICRO)*, 2009, pp. 14–23.

[47] A. Redaelli, D. Ielmini, U. Russo, and A. L. Lacaia, "Intrinsic data retention in nanoscaled phase-change memories-part ii: Statistical analysis and prediction of failure time," *IEEE Transactions on Electron Devices*, vol. 53, no. 12, pp. 3040–3046, Dec 2006.

[48] U. Russo, D. Ielmini, and A. L. Lacaia, "Analytical modeling of chalcogenide crystallization for pcm data-retention extrapolation," *IEEE Transactions on Electron Devices*, vol. 54, no. 10, pp. 2769–2777, 2007.

[49] U. Russo, D. Ielmini, A. Redaelli, and A. L. Lacaia, "Intrinsic data retention in nanoscaled phase-change memories-part i: Monte carlo model for crystallization and percolation," *IEEE Transactions on Electron Devices*, vol. 53, no. 12, pp. 3032–3039, Dec 2006.

[50] U. Russo, D. Ielmini, A. Redaelli, and A. L. Lacaia, "Modeling of programming and read performance in phase-change memories-part i: Cell optimization and scaling," *IEEE Transactions on Electron Devices*, vol. 55, no. 2, pp. 506–514, Feb 2008.

[51] U. Russo, D. Ielmini, A. Redaelli, and A. L. Lacaia, "Modeling of programming and read performance in phase-change memories-part ii: Program disturb and mixed-scaling approach," *IEEE Transactions on Electron Devices*, vol. 55, no. 2, pp. 515–522, Feb 2008.

[52] S. Schechter, G. H. Loh, K. Strauss, and D. Burger, "Use ecc, not ecc, for hard failures in resistive memories," in *Proceedings of the 37th Annual International Symposium on Computer Architecture (ISCA)*, ser. ISCA '10. New York, NY, USA: Association for Computing Machinery, 2010, p. 141–152. [Online]. Available: <https://doi.org/10.1145/1815961.1815980>

[53] N. H. Seong, D. H. Woo, and H. H. Lee, "Security refresh: Protecting phase-change memory against malicious wear out," *IEEE Micro*, vol. 31, no. 1, pp. 119–127, 2011.

[54] N. H. Seong, D. H. Woo, V. Srinivasan, J. A. Rivers, and H. S. Lee, "Safer: Stuck-at-fault error recovery for memories," in *2010 43rd Annual IEEE/ACM International Symposium on Microarchitecture (MICRO)*, 2010, pp. 115–124.

[55] N. H. Seong, S. Yeo, and H.-H. S. Lee, "Tri-level-cell phase change memory: Toward an efficient and reliable memory system," in *Proceedings of the 40th Annual International Symposium on Computer Architecture (ISCA)*, ser. ISCA '13. New York, NY, USA: Association for Computing Machinery, 2013, p. 440–451. [Online]. Available: <https://doi.org/10.1145/2485922.2485960>

[56] S. Shin, J. Tuck, and Y. Solihin, "Proteus: a flexible and fast software supported hardware logging approach for nvm," in *Proceedings of the 50th Annual International Symposium on Microarchitecture (MICRO)*, 2017, pp. 178–190.

[57] S. Sundararaman, N. Talagala, D. Das, A. Mudrankit, and D. Arteaga, "Towards software defined persistent memory: Rethinking software support for heterogeneous memory architectures," in *Proceedings of the 3rd Workshop on Interactions of NVM/FLASH with Operating Systems and Workloads (INFLOW)*, 2015, pp. 6:1–6:10.

[58] S. Swami and K. Mohanram, "Reliable nonvolatile memories: Techniques and measures," *IEEE Design Test*, vol. 34, no. 3, pp. 31–41, June 2017.

[59] S. Swami and K. Mohanram, "Adam: Architecture for write disturbance mitigation in scaled phase change memory," in *2018 Design, Automation Test in Europe Conference Exhibition (DATE)*, March 2018, pp. 1235–1240.

[60] S. Swami, P. M. Palangappa, and K. Mohanram, "Ecs: Error-correcting strings for lifetime improvements in nonvolatile memories," *ACM Transactions on Architecture and Code Optimization*, vol. 14, no. 4, 2017. [Online]. Available: <https://doi.org/10.1145/3151083>

[61] M. K. Tavana, A. K. Ziabari, M. Arjomand, M. Kandemir, C. Das, and D. Kaeli, "Remap: A reliability/endurance mechanism for advancing pcm," in *Proceedings of the International Symposium on Memory Systems*, ser. MEMSYS '17. New York, NY, USA: Association for Computing Machinery, 2017, p. 385–398. [Online]. Available: <https://doi.org/10.1145/3132402.3132421>

[62] J. Wang, X. Dong, and Y. Xie, "Point and discard: A hard-error-tolerant architecture for non-volatile last level caches," in *Proceedings of the 49th Annual Design Automation Conference (DAC)*, 2012, pp. 253–258.

[63] R. Wang, L. Jiang, Y. Zhang, L. Wang, and J. Yang, "Exploit imbalanced cell writes to mitigate write disturbance in dense phase change memory," in *Proceedings of the 52nd Annual Design Automation Conference (DAC)*, June 2015, pp. 1–6.

[64] R. Wang, L. Jiang, Y. Zhang, and J. Yang, "Sd-pcm: Constructing reliable super dense phase change memory under write disturbance," in *Proceedings of the 20th International Conference on Architectural Support for Programming Languages and Operating Systems*, ser. ASPLOS '15. New York, NY, USA: ACM, 2015, pp. 19–31. [Online]. Available: <http://doi.acm.org/10.1145/2694344.2694352>

[65] M. Weiland, H. Brunst, T. Quintino, N. Johnson, O. Iffrig, S. Smart, C. Herold, A. Bonanni, A. Jackson, and M. Parsons, "An early evaluation of intel's optane dc persistent memory module and its impact on high-performance scientific applications," in *Proceedings of the International Conference for High Performance Computing, Networking, Storage and Analysis*, ser. SC '19. New York, NY, USA: Association for Computing Machinery, 2019. [Online]. Available: <https://doi.org/10.1145/3295500.3356159>

[66] K. Wu, A. Arpacı-Dusseau, R. Arpacı-Dusseau, R. Sen, and K. Park, "Exploiting intel optane ssd for microsoft sql server," in *Proceedings of the 15th International Workshop on Data Management on New Hardware*, ser. DaMoN'19. New York, NY, USA: Association for Computing Machinery, 2019. [Online]. Available: <https://doi.org/10.1145/3329785.3329916>

[67] W. Xu and T. Zhang, "A time-aware fault tolerance scheme to improve reliability of multilevel phase-change memory in the presence of significant resistance drift," *IEEE Transactions on Very Large Scale Integration (VLSI) Systems*, vol. 19, no. 8, pp. 1357–1367, 2011.

[68] B. Yang, J. Lee, J. Kim, J. Cho, S. Lee, and B. Yu, "A low power phase-change random access memory using a data-comparison write scheme," in *Proceeding of the 2007 IEEE International Symposium on Circuits and Systems*, May 2007, pp. 3014–3017.

[69] J. Yang, B. Li, and D. J. Lilja, "Exploring performance characteristics of the optane 3d xpoint storage technology," *ACM Trans. Model. Perform. Eval. Comput. Syst.*, vol. 5, no. 1, Feb. 2020. [Online]. Available: <https://doi.org/10.1145/3372783>

[70] D. H. Yoon, J. Chang, R. S. Schreiber, and N. P. Jouppi, “Practical nonvolatile multilevel-cell phase change memory,” in *SC ’13: Proceedings of the International Conference on High Performance Computing, Networking, Storage and Analysis*, 2013, pp. 1–12.

[71] H. Yu and Y. Du, “Increasing endurance and security of phase-change memory with multi-way wear-leveling,” *IEEE Transactions on Computers*, vol. 63, no. 5, pp. 1157–1168, 2014.

[72] J. Yun, S. Lee, and S. Yoo, “Dynamic wear leveling for phase-change memories with endurance variations,” *IEEE Transactions on Very Large Scale Integration (VLSI) Systems*, vol. 23, no. 9, pp. 1604–1615, 2015.

[73] J. Zhang, D. Kline, L. Fang, R. Melhem, and A. K. Jones, “Dynamic partitioning to mitigate stuck-at faults in emerging memories,” in *2017 IEEE/ACM International Conference on Computer-Aided Design (ICCAD)*, 2017, pp. 651–658.

[74] L. Zhang, B. Neely, D. Franklin, D. Strukov, Y. Xie, and F. T. Chong, “Mellow writes: Extending lifetime in resistive memories through selective slow write backs,” in *Proceedings of the 43rd Annual International Symposium on Computer Architecture (ISCA)*, 2016, pp. 519–531.

[75] W. Zhang and T. Li, “Helmet: A resistance drift resilient architecture for multi-level cell phase change memory system,” in *Proceedings of the International Conference on Dependable Systems and Networks*, 07 2011, pp. 197 – 208.

[76] J. Zhao, S. Li, D. H. Yoon, Y. Xie, and N. P. Jouppi, “Kiln: Closing the performance gap between systems with and without persistence support,” in *Proceedings of the 46th International Symposium on Microarchitecture (MICRO)*, Dec 2013, pp. 421–432.

[77] P. Zhou, J. Y. B. Zhao, and Y. Zhang, “Throughput enhancement for phase change memories,” *IEEE Transactions on Computers*, vol. 63, pp. 2080–2093, 2014.